Brazilian Journal
of Chemical
Engineering

ISSN 0104-6632
Printed in Brazil
www.abeq.org.br/bjche

Vol. 25, No. 04, pp. 697 - 711, October - December, 2008

BEHAVIOR AND FLUIDIZATION OF THE COHESIVE POWDERS: AGGLOMERATES SIZES APPROACH

D. Turki[1*] and N. Fatah[2]

[1]Université Ibn-Khaldoun de Tiaret, Laboratoire de Chimie et Environnement,
BP 78, 14000 Tiaret, Algeria.
[2]Unité de Catalyse et de Chimie du Solide, UMR CNRS 8181, ENSC Lille,
bat. C7, 59655, Villeneuve d'Ascq Cedex, France.
E-mail: turkidjamel@yahoo.fr

(Received: August 01, 2007 ; Accepted: November 01, 2007)

Abstract - This work focuses on the fluidization of three types of TiO_2 powders: Anatase (99% TiO_2), Rutile 1 (95% TiO_2 and 5% Al) and Rutile 2 (96.5% TiO_2 and 3.5% Al and Si); the average diameters of the powders are 204 nm, 159 nm and 167 nm, respectively. These powders belong to group C of the Geldart classification and are characterized as cohesive powders with a non-free flow and a difficult fluidization. The fluidization of the powders was carried out in a glass column of 103 mm inner diameter and 1500 mm height. The experiments and analysis performed included measurements of the physical properties of the powders such as the particle size, density, specific surface area and the flow properties of the powders like the Hausner's index, the angle of repose, the angle of slide, consolidation and shearing (via shear cell testing). The results obtained with the nanometric TiO_2 powders show a more complex behavior than the micronic powders; with a low strength value (Hausner index, angle of repose and angle of slide), the TiO_2 powders have a free flow or intermediate-flow and a non-free-flow for higher strength intensities (consolidation and shearing). This behavior is related to the structure of the nanometric particles in the packed bed; the evolution of this structure is made up of individualized and spherical agglomerate shapes and is not perturbed by stresses of low intensities. Indeed, the latter seems to modify the structure of the powder (group C of Geldart classification) to acquire a behavior typical of group A, B or D in the Geldart classification. With high stress values, the individualized agglomerates are disintegrated and the powder is reduced to a more compact structure. The fluidization of TiO_2 powders seems to evolve in a more homogeneous way than the micronic powders. This behavior is related to the initial structure being made up of stable agglomerates. Thus, this fluidization is made by agglomerates with a gas velocity of 3×10^6 to 4.6×10^6 times the gas velocity for fluidizing the primary particles.A numerical approach based on a force balance in agglomerating fluidized beds was developed in order to estimate the agglomerates sizes.
Keywords: Fluidization; Cohesive powder; Agglomerate; Nanometric powder; Interparticle Forces.

INTRODUCTION

In the last years, fluidization has progressed through systematic research, with various specialized functions such as: combustion, mixing, chemical reaction, heat and mass transfer, coating, granulation, encapsulation and CVD (Chemical Vapor Deposition) processes. This research development persuaded the researchers to become interested in the use of fine powders (cohesive powder), micronic and nanometric powders. Many industrial processes require the use of fine powders in the manufacture of catalysts for reactors, ceramics, pharmaceuticals, paints and cosmetics.

According to research performed for nearly fifty years, the fluidization of fine powders (diameter of the primary particles less than 50 μm) is complex. The difficulty of putting these powders in suspension

*To whom correspondence should be addressed

in the fluidizing gas is related to the cohesive structure and, in particular, to the physical forces between the primary particles. In general, the experiments are complex during the handling or fluidizing of these powders. This is due to the unpredictable behaviors of the cohesive powders. This category of powders belongs to group C of Geldart's classification (Geldart, 1973). The complexity of this behavior is due to the small size of the fine particles, i.e., the micronic or nanometric particles. These tend to form agglomerates (self-agglomeration) of completely random size and shape by the action of the interparticle forces between the primary particles. This is related to the high ratio between the surface and the volume of the particles and to the short distance between the particles. This strong interaction between the powders affects the flow properties of the powders.

The smooth fluidization of gas-solid particles is the result of equilibrium between the hydrodynamic, gravitational and interparticle forces. However, in the case of cohesive powders, the interparticle forces are considerable and they control the behavior of a bed composed of fine particles. Thus, during fluidization, the bed of powder cracks into large portions and the gas tends to flow into the gap between the fissures. Then, channeling occurs in the bed and, eventually, the gas-solid contact is very low and any heat and mass transfer operation is weakened.

The powders are generally presented in the form of heterogeneous structures in particle size, size distribution, morphology (shape) and physical properties (density, specific surface area and porosity). These characteristics are related to the local structure of the particulate system and the type of gas flowing around these particles. In the case of the cohesive powders, this particulate system appears to be very complex and uncontrollable. The interparticle forces are considerable and control the micronic and nanometric particle behavior of the bed. This physical attraction is the effect of the great intensity of internal forces between primary particles. In the case where the particulate system is handled in air and when the size and the distance between the particles are very small, the van der Waals forces are controlling rather than the other interactions forces (capillary and electrostatic forces). The particle-particle interactions are achieved primarily by contact. If the particles are not in contact, no force is exerted between them. The van der Waals forces between two macroscopic bodies are calculated in a different way from the microscopic one. Indeed, the force of interaction between two solids depends on the size, the shape and the roughness of the particles, as well as the distance between the particles. These forces are calculated starting from the Derjaguin approximation (Derjaguin, 1934) and the theory of Lifshitz (Lifshitz, 1956). The estimation of the van der Waals forces is defined as the sum of all interactions between molecules held on the surface of the particles face to face. The magnitude of these forces increases with the size reduction of the particles and becomes dominating compared to the weight of the particles.

In many industrial processes, the cohesive powders are fluidized in the form of agglomerates. For this, it is necessary to apply either a high gas velocity (Fatah and Cavrois, 1998) compared to the velocity necessary for fluidizing primary particles, or a lower velocity but with addition of external energy. (Chirone et al., 1993) drew up a list of techniques used as additional energy (vibration, magnetic pulsation and acoustic energy) to disintegrate the cohesive structure and to facilitate the fluidization of the agglomerates. The mechanism of agglomerate fluidization supposes the passage from group C to a group A powder or even a group B powder of the Geldart classification. (Leu and Huang, 1994) note a clear improvement of the quality of fluidization and expansion of the bed for powders with low particle size under the effect of the acoustic pressure. Indeed, this seems to modify (Russo and al., 1995) the structure of the fluidized bed (group C of Geldart) and to acquire a behavior typical of group A of Geldart. (Nezzal, 1996) describes that the use of mechanical agitation (intrusive method) modifies the hydrodynamic behavior of the bed powder. This provides a better aeration of the bed particles and homogenizes the fluidization in the form of agglomerates. Thus, the size of the agglomerates decreases when the agitating velocity increases.

The aim of this work is to study an important feature of powder structure and the use of different measurement techniques that can help to understand the behavior of fine particles. The experiments and analysis performed included measurements of the physical properties of the powders such as the particle size, density, specific surface area and the flow properties of the powders like the Hausner's index, the angle of repose, the angle of slide, the consolidation and the shearing (via annular shear cell).

The flowability and the physical properties of the powders seem to be an interesting way of describing the hydrodynamic behavior of the very cohesive structure.

The interparticle forces for the cohesive interaction are determined by a force balance (kinetic, van der Waals, collision, gravitational and buoyancy forces). A numerical approach based on a force balance in agglomerating fluidized beds was developed in order to estimate the agglomerate's sizes.

The experimental results indicate that there is a close correlation between the hydrodynamics and the local structure of the powder bed.

MATERIALS AND METHODS

In this work three types of TiO_2 powders of the Kronos company were studied:

- Anatase (99% TiO_2): labeled TiO_2 (A);
- Rutile1 (95% TiO_2 and −5% Al): labeled TiO_2 (R1);
- Rutile2 (96.5% TiO_2 and −3.5% Al and Si): labeled TiO_2 (R2).

The powder size distribution was measured with the light-scattering laser instrument (Beckman-Coulter, LS230). This experiment measures the particle size. It should be noted that, due to the complexity of this experiment, each batch of powder was analyzed according to a suitable protocol that gives the primary particle size and not the size of agglomerate. During these experiments, the optimal conditions obtained to reach the lowest size of TiO_2 particles without degrading the powder structure, are as follows: the cohesive powders were dispersed in demineralised water with addition of 0.5% tetrasodium diphosphate as dispersant in a flask. Before the introduction of this suspension into the laser instrument and for a better dispersion of the primary particles, a manual mixing of TiO_2 (R1) powders and the use of ultrasound for TiO_2 (A) and TiO_2 (R2) was carried out in a flask. The average diameter of the three powders of TiO_2 was calculated according to the diameter definition "surface-volume" or Sauter diameter:

$$d_p = \frac{\sum N_i d_i^3}{\sum N_i d_i^2} \quad (1)$$

where N_i is the number of particles in class i and d_i the average diameter of the particle in this class.

The range of the particle size distribution was quantified using the index of uniformity C_u (Schlosser, 1998) obtained from the cumulative percentage undersize curve (in volume) and defined by the following equation:

$$C_u = \frac{d_{i\,60\%}}{d_{i\,10\%}} \quad (2)$$

$C_u < 2$: The particle size distribution is known as uniform.

$C_u > 2$: The particle size distribution is known as non-uniform or large.

$d_{i60\%}$ and $d_{i10\%}$ are defined as dimensions of the particles corresponding respectively to 60% and 10% of the particle size distribution of the cumulative curve.

The density (ψ_p) and the BET surface area (S_s) of powders were, respectively, measured by helium gas pycnometer (Micromeritics, AccuPyc 1330) and nitrogen gas adsorption (Micromeritics, Asap 2000).

MEASUREMENTS OF FLOW PROPERTIES

Measurements were carried out under the same working conditions, i.e., with a relative humidity ranging between 40% and 53% and at ambient temperature. The tests were carried out according to a specific protocol in order to preserve the reproducibility of the results. With regard to the following techniques:

- Ensuring that the initial structure of particles is homogeneous during filling. In this test, the loading of powder is carried out with a vibrating sieve of 1 mm in aperture.
- Using a smooth and clean cell wall to decrease friction forces and contamination of the powder.
- Controlling humidity related to each test, to avoid capillary interactions.

For most measured flow properties, the average of 10 successive measurements was recorded except for the test of shearing, where measurements were repeated three times. Table 1 shows the average flow measurements and the standard deviation representing the average error of these measurements.

Hausner's Index

The Hausner index (HR) is defined as the ratio of bulk density ψ_t of fine powders after prolonged tapping to aerated density ψ_{ae}.

$$HR = \frac{\psi_t}{\psi_{ae}} \quad (3)$$

HR describes the powder flowability. The various flows can be classified as follows:

HR > 1.4 characterizes cohesive powders (non-free flowing), HR < 1.2 indicates a free flowing (non-cohesive powders) and 1.2 < HR < 1.4 shows an intermediate behavior of the powders. This test measures the reduction of the volume of packed bed of particles. This is carried out in a graduated cylinder of 100 ml. The initial volume of the particles is fixed at 40 ml. Finally, the cylinder is subjected to vertical tapping until no change in the volume related to time is observed. The packed volume of the powders is recorded when that volume remains constant with time. The tapping technique was achieved using two methods: manual (manual tapping of the powder in a test-tube) and automatic with an ERWEKA SVM22 device.

Angle of Repose Measurement

The angle of repose (ζ) was measured by applying the flow procedure through a funnel. This measurement consists of passing a known mass of powder through a funnel with a sieve of 1mm in aperture and 35 mm in diameter, the funnel is submitted to a mechanical vibration to form a uniform powder heap on a glass base of 40 mm in diameter. The funnel is fixed at a distance of 45 mm from the base. The angle of repose is the constant angle formed by the base and the tangent to the heap formed by the powder. The flow is known as free flowing for ζ < 40° and non-free for ζ > 40°.

Angle of Slide Measurement

The device for measurement of the angle of slide (η) is composed of a glass plate 40 mm in width, 145 mm in length and 5 mm thick revolving around a hinge of 0° to 180° from a fixed support (Figure 1). After depositing a uniform particle layer 5 mm thick, gradually we inclined the plate at a practically constant velocity until no particle is on the surface plate (or covered of a mono-layer of particles that adhere to the wall). The slide angle is the angle formed by the plate and the fixed support. The flow is known as free for η < 30° and non-free for η > 30°.

Consolidation Test

The consolidation test shows the aptitude that a powder has to consolidate, i.e., to decrease the volume of the packed bed of powder under the effect of an increasing normal stress (ω). A known mass of powder (M) is introduced into a graduated 5.3 cm diameter cylinder. The base of the cylinder is closed by a porous plate to allow the evacuation of the air stored in the powder during consolidation. A twister is introduced into the cylinder to homogenize the surface of the powder. A glass piston is applied on the powder and the variation of volume is measured according to the force (F) related to the cylinder (Figure 2). The solid fraction (1- κ) related to the strain ω is noted as:

$$1-\kappa = \frac{M}{\rho_p V_t} \tag{4}$$

M and V_t are the mass and the total volume of the packed bed of particles, respectively.

$$\omega = \frac{F}{S} \tag{5}$$

S is the cross-sectional area of the glass piston.

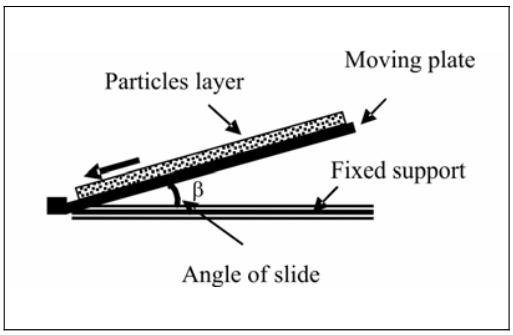

Figure 1: Device measurement of the angle of slide

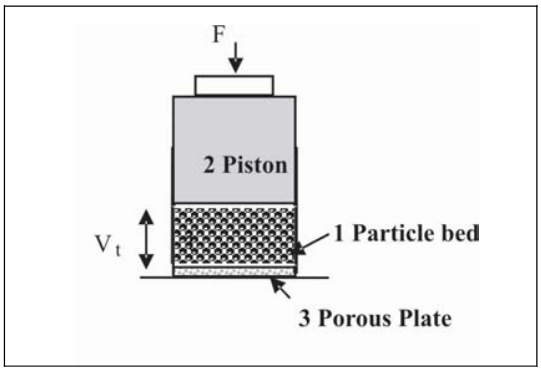

Figure 2 : Consolidation test

Annular Shearing Cell

The annular shear cell (RST-XS) (Schulze, 1995) is an alternative version of Jenike's cell (Jenike, 1954). The illustration follows the same procedure and theory as Jenike's cell (Jenike, 1954), where the yield locus is obtained starting from at least four characteristic points of rupture for a given consolidation state. With the annular shearing cell, a complete yield locus is usually measured with one sample (in contrast to the Jenike shear tester where only one point can be measured with one sample). This cell is automatic and less time consuming.

The shearing test (annular cell) is composed of an annular channel, carefully filled with the powders. A lid is placed on the annular channel and the unit is then placed on a revolving plate. Then a piston is lowered on the lid. The lid has as the role of transmitting at the normal strain (ω) and the shear stress (ϑ) simultaneously to the powder. Only the lower plate is in rotation and engages the annular channel (Figure 3). The upper part, i.e., the lid, is maintained fixed using two tie rods transmitting the shearing force to the sensors. The first stage consists of shearing the powder until a stationary state corresponding to a plate marking the flow, then the cell returns to its initial state. In this case the critical point (stationary flow) is reached ($\omega_{sf},\vartheta_{sf}$) in the coordinate system (ω, ϑ) (Figure 4), i.e., the limiting point of flow. The second point in this same system is obtained by applying ω { ω_{sf} and the powder is sheared until rupture that corresponds to the start of flow, the value of ϑ is noted and the second point (ω, ϑ) is obtained. The whole procedure is repeated for three or four other points. The curve, called yield locus (Figure 4), is obtained. This illustrates the limit between two zones corresponding to the pressures applied: the zone in the lower part of the yield locus corresponds to an impossible flow of the powders and the zone above the yield locus curve represents the collapse of the powder and flow.

From the yield locus two properties of flow can be obtained:

Á The cohesion C is the value of the ordinate at the origin (ω=0). This parameter gives the true cohesion between the particles apart from particle-particle friction. For C=0, the powder shows a free flow; for C > 0 the powder is said to have a non-free flow.

Á The compressive resistance F_c is obtained from Mohr's circle passing through the origin and tangent to the yield locus.

Á The principal stress ω_8 corresponds to the maximum stress that the powder has undergone for the first time. It is obtained from Mohr's circle passing through the point ($\omega_{sf},\vartheta_{sf}$) and tangent to the yield locus.

From the values of ω_1 and F_c, the parameter $FF_c = \omega_1/F_c$ can be defined and this characterizes the flow property of the powders according to the following classification:

Á $FF_c < 2$: very cohesive powder, non-free flow.

Á $2 < FF_c < 4$: cohesive powder, difficult flow.

Á $4 < FF_c < 10$: intermediate flow.

Á $10 < FF_c$: non cohesive powder and free flow.

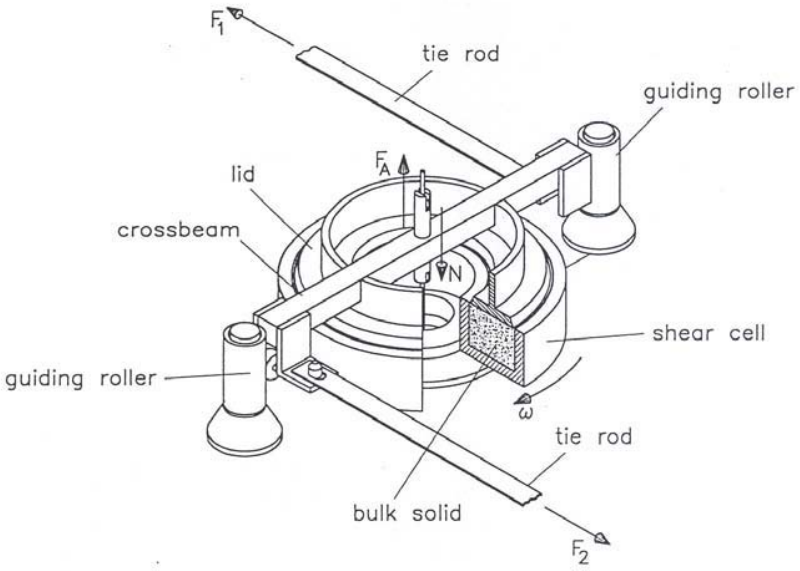

Figure 3: Annular shearing cell (Schulze, 1995)

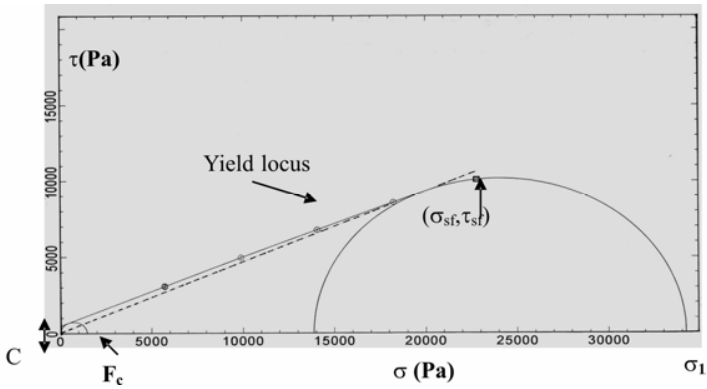

Figure 4: Determination of the yield locus

EXPERIMENTAL APPARATUS: FLUIDIZATION COLUMN

The tests of fluidization were carried out in a glass column of 103 mm inner diameter and 1500 mm height (Figure 5). Air was used as the fluidizing gas; the flow was controlled by a set of rotameters. The diffusion of air through the bed of particles is ensured by using a porous stainless steel plate (gas distributor) placed at the base of the column. The filtering capacity of the porous plate is 98 % and 99.9 % to stop particles of 1.2 µm and 3.6 µm in size, respectively. The pressure drop (÷P) through the bed is measured using a pressure probe made up of a stainless steel tube of 1mm inner diameter, immersed in the column and placed just above the distributor. To avoid clogging the pressure probe by fine powders, the end of this tube is protected by a double steel sheet of 50 µm in aperture. The tube is connected to a differential pressure sensor (Societé Sedeme) where the second pressure probe corresponds to atmospheric pressure. The fluctuation of the recorded pressure drop (÷P) with time and velocity of the gas are achieved using a Sefram recorder. A cyclone is connected to the top of the column to collect the fine particles elutriated during fluidization.

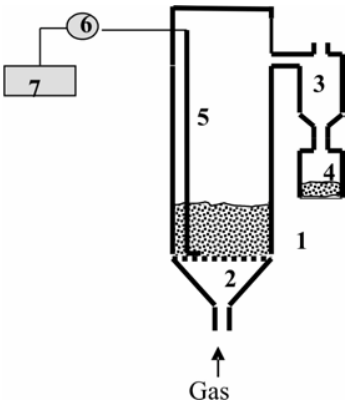

1. cylindrical fluidized bed
2. gas distributor
3. cyclone
4. collecting bottle
5. pressure probe
6. differential pressure sensor
7. recorder

Figure 5: Fluidization column

RESULTS AND DISCUSSION

The studies of the cohesive powders (Fatah et al., 1998; Fatah and Sanchez, 2004) reveal the existence of two categories of powders: micronic particles (diameter of the particle varying between a value of − 500 nm and − 50 µm) and nanometric particles (diameter of the particle less than − 500 nm). The nanometric particles are more complex and show a different behavior from the micronic particles under the action of the variation of the external forces. Thus, this present work is concentrated on the study of the behavior of nanometric powders.

The particle size distributions of the three TiO_2 powders were obtained according to an optimal procedure of dispersion in order to measure the size of the primary particles and not that of agglomerates. The particle size distributions of the TiO_2 powders are given in Figure 6. The average sizes of the particles are d_p=204 nm, d_p=159 nm and d_p=167 nm for TiO_2 (A), TiO_2 (R1) and TiO_2 (R2), respectively. The C_u index is obtained from the cumulative percentage curve and defined by equation (2). This parameter indicates a broad size distribution corresponding to Cu= 3.6, Cu=3 and Cu= 3 for the three TiO_2 powders (TiO_2 (A), TiO_2 (R1) and TiO_2 (R2)), respectively. This large interval is due to the presence of agglomerates, as shown in Figure 6. For the three powders, a first mode towards 225 nm is observed, that seems rather close to the average diameter calculated.

The particle density ($ρ_p$) is 3900 kg/m^3, 4200 kg/m^3 and 4200 kg/m^3 for TiO_2 (A), TiO_2 (R1) and TiO_2 (R2), respectively. The BET surface area seems to be identical for the three powders and is about 9 m^2/g.

Table 1: Flow property values and standard deviation of TiO_2 powders

Powder	Hausner index HR		Angle of repose	Angle of slide	Standard deviation			
	automatic	manual	Ŭ(°)	ɓ(°)	HR		Ŭ	ɓ
					automatic	manual		
TiO_2 (A)	1.27	1.60	51.0	37.4	0.014	0.059	1.26	6.75
TiO_2 (R1)	1.28	1.77	43.5	43.8	0.020	0.050	1.00	6.80
TiO_2 (R2)	1.23	1.65	41.7	37.7	0.050	0.050	1.22	2.42

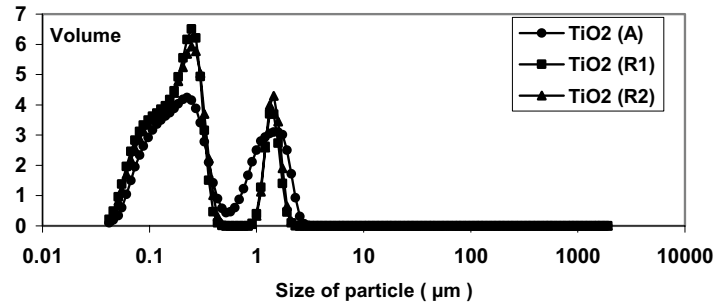

Figure 6: Size distribution of TiO_2 (A), TiO_2 (R1) and TiO_2 (R2)

The study of TiO_2 powder flows shows a free to intermediary flow under the action of low strength, i.e., in the case of using the automatic tapping test measurement (Hausner's index, angle of repose and angle of slide) (Figures 7, 8 and 9) and Table 1. The values of HR seem to be identical and slightly higher than 1.2. It is the same for the angle of repose and the angle of slide, which are close to 41°-51° and 37°-43°, respectively. This behavior is related to the initial structure of the nanometric powder in the packed bed that appears to be (visually) made up of stable agglomerates with different diameters and close to a spherical shape. This structure seems to depend on the history of the packed bed (self-agglomeration) and the process of micro-consolidation. This phenomenon is due to the great intensity of the interparticle forces and to the very short distance between primary particles. Such a structure generates a number of agglomerates with a large size distribution that can be classified in group A, B or D of Geldart's classification. Finally, this powder system does not seem to evolve under the action of forces with low intensities.

However the application of higher forces by manual tapping test, consolidation test and annular shear cell, indicates a non-free flow (Figures 7, 10 and 11). The values of HR are much higher than 1.4 (results more coherent for this type of powders) and do not seem to evolve identically for powders when using automatic tapping. It is more advisable to link this test with consolidation and shearing tests to categorize the powders Thus, it is noted that the powders do not present the same degree of cohesion.

Figure 10 shows the variation of the solid fraction (1-Ů) according to the normal strain (ω) (test of consolidation). In the initial state, a high rate of aeration is noted, indicating a solid fraction of about 15%, 18% and 19% for TiO_2 (A), TiO_2 (R1) and TiO_2 (R2), respectively, and formation of porous agglomerates with an internal porosity ε. Experimental error for the calculation of the solid fractions came from the estimation of the standard deviation. Thus, values of 0.029, 0.0419 and 0.050 are obtained for TiO_2 (A), TiO_2 (R1) and TiO_2 (R2) powders, respectively. Then, for a low consolidation, (1-Ů) increases with ω, according to a slightly linear evolution. This corresponds to the diffusion of air in the structure of the packed bed of particles. For higher values of ω, the transition zone is reached, corresponding to the load held by the solid structure; then packing and rearrangement of the particles occurs. Beyond this zone, the load is spread out on the solid; thus, there is consolidation of the packed bed of powder. Low solid fraction values (in the case of TiO_2 (A)) show a very cohesive behavior of the powders. However, TiO_2 (R1) powder seems to be less cohesive than TiO_2 (A) and TiO_2 (R2) powders. In the same way, Figure 11 represents experimental results obtained from the annular shear cell, where the FF_c value characterizes the type of flow (deformation of the powder's packed bed) and C indicates cohesion between particles. For all powders, the results indicate a non-free flow ($FF_c < 2$ and $C > 0$). The TiO_2 (A) and TiO_2 (R2) powders show higher degrees of cohesion than TiO_2 (R1). These results are in perfect agreement with those obtained with the test of consolidation. However, they seem to be in contradiction with the results obtained when using the manual tapping test, due to the fact that the stress applied with this test still remains low compared to the test of consolidation and shearing. This phenomenon shows that the study of nanometric powders should be carried out with care. Thus, it is sensible to link several tests.

In this work, the TiO_2 powder structure loses its individualized character (formation of dispersed agglomerates) under the action of high values of external force. Thus, there is a rupture of agglomerates and the structure changes to a more compact powder system, identical to a dense bulk that makes the handling of these powders very complex. The cohesive character of these powders is detectable only under high external forces that overcome the effect of the internal forces between particles that form agglomerates.

Thus, to fluidize the TiO_2 powders, an important energy must be applied not only to disintegrate the cohesive structure but also to set in suspension the agglomerates. Referring to these results the TiO_2 (R1) powder should be fluidized with a gas velocity lower than the two other powders.

The suspension of the TiO_2 powders was carried out with air and at ambient temperature. The disintegration of the cohesive structure in the fluidized bed was carried out under high gas velocity (å 0.5m/s).

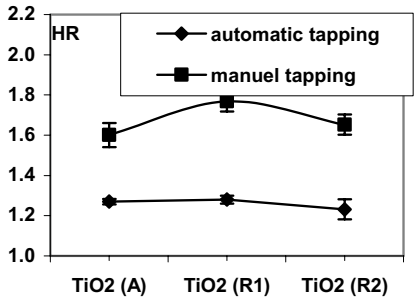

Figure 7: HR evolution for the three TiO_2 powders: automatic and manual tapping

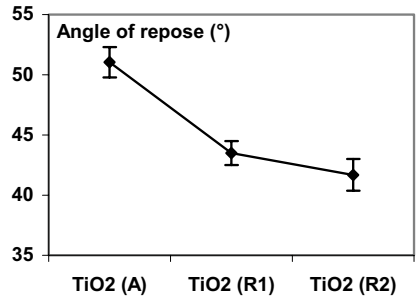

Figure 8: Evolution of the angle of repose for the three TiO_2 powders

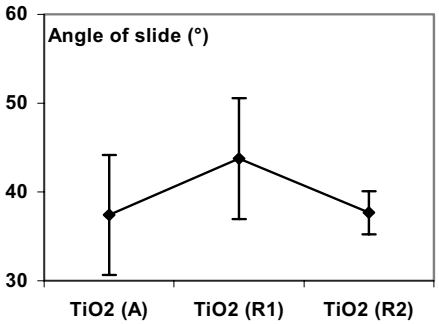

Figure 9: Evolution of the angle of slide for the three TiO_2 powders

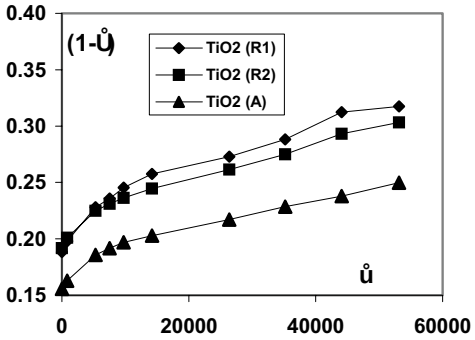

Figure 10: Variation of the solid fraction according to the normal strain for the three TiO_2 powders

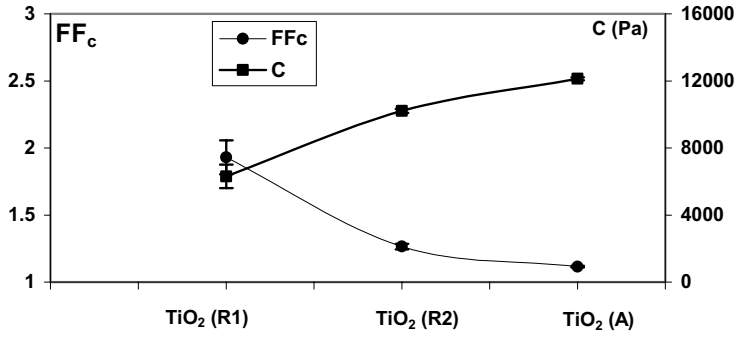

Figure 11: Evolution of FF_c (flow characteristic) and C (cohesion) for the three TiO_2 powders

During the fluidization of Geldart's group C powders, the following phases often observed can be listed below:

1) For low gas velocity, the fluid crosses the cohesive structure by creating a preferential passage (channeling). The totality of the gas passes through a channel, observed especially for beds that are not deep enough (the static height of the bed of particles lower or equal to the diameter of the column). For deep beds, the channeling is preceded by the appearance of the phenomenon of slugging. This same behavior was observed by (Pacek and Nienow, 1990).

2) For higher gas velocity, the formation of cracks and channels at various orientations is observed and does not seem to be reproducible.

3) A defluidization is noted in the bottom zone of the bed but, beyond this, a pseudo-fluidization is observed as if the various channels formed acted as gas jets. On top of the jet there is formation of bubbles (behavior similar to a spouting bed) that maintains this zone in fluidization. The bottom zone of the bed seems to be reduced with increasing gas velocity to form a structure made up of agglomerates.

During fluidization of the three types of TiO_2 powders, only phase 2 and phase 3 were observed for gas velocities much higher than the necessary fluidization velocity of the primary particles. This high velocity disintegrates the cohesive structure and eases the fluidization of agglomerates.

For the TiO_2 powders, the preferential passage of the gas through the bed of particles seems to be non-existent; this is due to the initial structure of the TiO_2 powder bed formed by individualized agglomerates (self-agglomeration). Figure 12 illustrates all the curves related to the variation of the pressure drop (÷P) according to the gas velocity (U) for the three powders (TiO_2 (A), TiO_2 (R1) and TiO_2 (R2)).

Fluidization of cohesive powder highlights the suspension of the agglomerates at a very high gas velocity (above the minimum velocity). Thus, the cohesive powders are arranged to form a new structure of agglomerates (made up of primary particles). The apparent minimum fluidization velocity (U_{mfa}) has been determined approximately from the third zone by the standardized method of Richardson (Richardson, 1971), that corresponds to the intersection with the horizontal line (fluidization of agglomerates) and the relative curve of the bed that exhibits the formation of cracks at different orientations. The horizontal line and the relative curve are estimated with a regression analysis to fit approximately the corresponding values. As an example, Figure13 illustrates the determination of the apparent minimum fluidization velocity (U_{mfa}) of T_iO_2 (A). Values of 0.176 m/s, 0.11 m/s and 0.175 m/s for the TiO_2 (A), TiO_2 (R1) and TiO_2 (R2) powders are noted, respectively. The results are compared with those of references to calculate the fluidization index defined as the ratio between U_{mfa} and the fluidization velocity calculated (U_{mfc}) from the (Wen and Yu, 1966) correlation.

$$U_{mfc} = \frac{d_p^2 g(\rho_p - \rho_g)}{1650\mu_g} \quad (6)$$

where σ_g and ψ_g indicate the viscosity and the density of the air, respectively.

However, it is important to note that the minimum fluidization velocity (U_{mfc}) is calculated from the physical properties of the primary particles: TiO_2 (A) (d_p=204 nm and ψ_p=3900 kg/m^3), TiO_2 (R1) (d_p=159 nm and ψ_p=4200 kg/m^3) and TiO_2 (R2) (d_p=167 nm and ψ_p=4200 kg/m^3). That is around 5.2 $\Delta 10^{-8}$ m/s, 3.4$\Delta 10^{-8}$ m/s and 3.76$\Delta 10^{-8}$ m/s for TiO_2 (A), TiO_2 (R1) and TiO_2 (R2), respectively. Finally, the index of fluidization (U_{mfa}/U_{mfc}) is about 3.4$\Delta 10^6$, 3.2$\Delta 10^6$ and 4.6$\Delta 10^6$ for TiO_2 (A), TiO_2 (R1) and TiO_2 (R2), respectively. These results indicate that it is necessary to inject a gas velocity about 4$\Delta 10^6$ times higher than the velocity (U_{mfc}) necessary to fluidize the primary particles for the three powders. In addition, the dynamic diameter of the agglomerates, d_{pa}, was estimated using equation (6) according to the minimum gas velocity of the experimental fluidization or U_{mfa}. Values of d_{pa}=375 µm, d_{pa}=285 µm and d_{pa}=360 µm were obtained, i.e., 1838, 1792 and 2155 times larger than the diameter of the primary particles (d_p) for the three powders TiO_2 (A), TiO_2 (R1) and TiO_2 (R2), respectively.

Supposing that the agglomerates thus formed are porous, this implies that the density of the agglomerate (ψ_a) is less than that (ψ_p) of the primary particles. A simple calculation of ψ_a (ψ_a# #ψ_p (1-з›)) can be done by estimating the internal porosity (•) of the agglomerates (the mean value bed powder porosity between tapped and aerated treatment of the bulk powder bed). Thus, values of 0.8, 0.75 and 0.76 were obtained for TiO_2 (A), TiO_2 (R1) and TiO_2 (R2)), respectively. The corresponding agglomerate densities (ψ_a) for the three powder of TiO_2 are 780 kg/m^3, 1050 kg/m^3 and 1029 kg/m^3 for TiO_2 (A), TiO_2 (R1) and TiO_2 (R2), respectively. Taking into account the dynamic diameter of the agglomerates (d_{pa}) and the values of ψ_a, this hydrodynamic behavior for the three powders can be classified in group B of Geldart's classification.

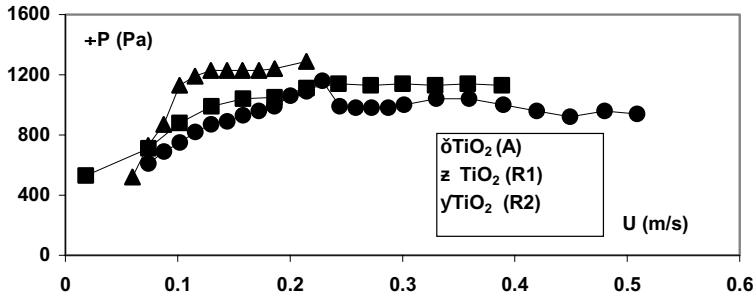

Figure 12: Pressure drop variation versus superficial gas velocity for the three TiO_2 powders

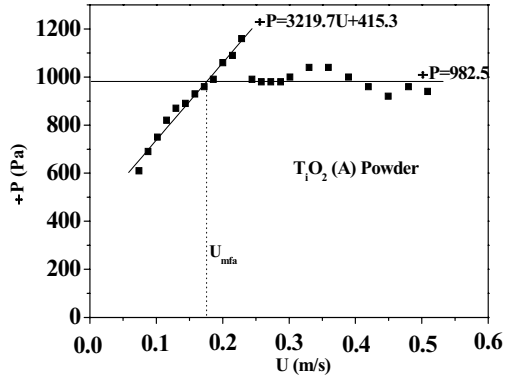

Figure 13: The determination of the apparent minimum fluidization velocity (U_{mfa}) of T_iO_2 (A)

A model is developed to estimate the agglomerate size in a fluidized bed, taking into account the various forces that control the formation of agglomerates in this bed of Geldart's group C powders, and assuming that cohesiveness is principally due to van der Waals forces rather than the other interaction forces (capillary and electrostatic forces).

The forces acting on an agglomerate in a fluidized bed are determined by the force balance (Zhou and Li, 1999):

Drag force(F_y)+Collision force(F_{co}) = Gravitational - Buoyancy force(F_g)+Cohesive force (F_{va}).

The drag force exerted by a fluid with density J_g and a superficial gas velocity (U) flowing past an isolated agglomerate of diameter (d_a) is given by:

$$F_y = \frac{1}{2} C_d z J_g U^2 \quad (7)$$

where $z = \frac{´.d_a^2}{4}$ is the projected area of the sphere and C_d is the drag coefficient; this coefficient depends on the Reynolds number (Re). Significant research has been done on flow past fixed and fluidized beds and it is possible to calculate drag forces over agglomerates in the bulk of a uniform suspension of agglomerates with reasonable accuracy. The corresponding drag force according to (Khan and Richardson, 1990) is given by:

$$F_y = 0.055 ´ J_g d_a^2 U^2 Ů^{4.8} \quad (8)$$

where (d_a) is the agglomerate diameter and Ů is the fluidized bed voidage.

The collision force between two agglomerates '1' and '2' vertically aligned in a fluidized bed that collide inelastically with a relative velocity (q) is according to (Timoshenko and Goodier, 1970), given by:

$$F_{co} = n \, Ŭ_d^{\frac{3}{2}} \quad (9)$$

where $Ŭ_d$ is the displacement of the maximum compression and is given by:

$$\breve{U}_d = \left(\frac{5}{4} \frac{q^2}{n\, n_1} \right)^{0.4} \quad (10)$$

The parameters n and n_1 are expressed by:

$$n = \sqrt{\frac{8}{9\pi^2 / k_1 + k_2 \breve{0}^2} \frac{d_{a1}\, d_{a2}}{d_{a1} + d_{a2}}} \quad (11)$$

and

$$n_1 = \frac{m_1 + m_2}{m_1\, m_2} \quad (11a)$$

where m_1 and m_2 are the masses and d_{a1} and d_{a2} are the diameters of agglomerates '1' and '2' respectively, k is a function of Poisson's ratio and Young's modulus. Since the two agglomerates are assumed to have the same properties, then $m_1=m_2=m$ and $k_1=k_2=k$ and therefore:

$$\breve{U}_d = \left(\frac{5}{8} \frac{q^2 \pi^2 k \rho_a d_{a1}^3\, d_{a2}^3}{(d_{a1}^3 + d_{a2}^3)} \sqrt{\frac{d_{a1} + d_{a2}}{2\, d_{a1}\, d_{a2}}} \right)^{0.4} \quad (12)$$

where ρ_a is the density of agglomerate estimated by measuring the internal porosity of the agglomerate (mean value powder bed porosity between tapped and aerated powder). The factor k is given by (Timoshenko and Goodier, 1970).

$$k = \frac{1-\sigma^2}{\pi E} \quad (13)$$

where σ is the Poisson's ratio and E is the Young's modulus.

Substituting equations (12) and (11) into equation (9) we obtain:

$$F_{co} = n \breve{U}_d^{\frac{3}{2}} = 0.2516 \left(\frac{\pi q^6 \rho_a^3}{k^2} \left(\frac{d_{a1}^3 d_{a2}^3}{d_{a1}^3 + d_{a2}^3} \right)^3 \left(\frac{2\, d_{a1}\, d_{a2}}{d_{a1} + d_{a2}} \right)^3 \right)^{0.2} \quad (14)$$

If $d_{a1}=d_{a2}=d_a$ then

$$F_{co} = 0.166 \left(\frac{q^6 \rho_a^3}{k^2} \right)^{0.2} d_a^2 \quad (15)$$

The difference in gravitational and buoyancy forces acting on one agglomerate can be expressed by:

$$F_g = \frac{\pi}{6} (\rho_a - \rho_g) d_a^3\, g \quad (16)$$

The cohesive force is controlled mainly by the van der Waals force, given by (Derjaguin, 1934) as:

$$F_{va} = \frac{A}{12 \breve{u}^2} \frac{d_{a1}\, d_{a2}}{d_{a1} + d_{a2}} \quad (17)$$

where $\breve{u}$ is the distance between the agglomerates' surfaces and A is the Hamaker constant. According to (Israelachvili, 1985), this constant can be evaluated when the medium is a vacuum from:

$$A = \frac{3}{4} B T \left(\frac{\varepsilon_1 - 1}{\varepsilon_1 + 1} \right)^2 + \frac{3 h \nu_e}{16\sqrt{2}} \frac{(N_1^2 - 1)^2}{(N_1^2 + 1)^{1.5}} \quad (18)$$

where h is Plank's constant, B is Boltzmann's constant, T is the absolute temperature, N_1 is the index of refraction of the particles and ν_e is the UV adsorption frequency.

Taking $d_{a1}=d_{a2}=d_a$ and substituting these equations into the force balance equation we have:

$$(\rho_a - \rho_g) g d_a^2 - \left(0.33 \rho_g U^2 \varepsilon_f^{4.8} + 0.3172 \left(\frac{q^6 \rho_a^3}{k^2} \right)^{0.2} \right) d_a + \frac{A}{4\pi \breve{u}^2} = 0 \quad (19)$$

It has been observed that the significant parameters that disturb the solution of equation (19) are: the density of the agglomerates and the fluid, the relative collision velocity and the distance between the agglomerate surfaces. The solution of equation (19) depends on the exact estimation of the parameters, so some parameters have been experimentally obtained from different powders of TiO_2: ε_f (fluidized bed porosities), ρ_a (densities of agglomerates), U (superficial gas velocities, as explained above). For TiO_2 powders, the parameters:

N_1, κ_1, ε_c, B and h are obtained from (Perry and Green, 1984; Israelachvili, 1985), where h is Plank's constant $h=6.626\times10^{-34}$ J.s and B Boltzmann's constant $B=1.381\times10^{-23}$J/K. The index of refraction (N_1) and the dielectric constant (κ_1) of TiO_2 particles are 2.493 and 40-60, respectively. The UV adsorption frequency is $\varepsilon_c=3\times10^{15}$ s^{-1}. With an absolute ambient temperature, the Hamaker (A) constant calculated from equation (18) is $A=3.97\times10^{-19}$ J. The distance between agglomerate surfaces ($\breve{u}$) is taken as 4×10^{-10} m (Krupp, 1967). The parameter k calculated with Poisson's ratio and Young's modulus is $k=3.0\times10^{-06}$ Pa^{-1} (Krupp, 1967).

For an estimated porosity $\kappa = \kappa_{aerated}$ ($\kappa = \kappa_{aerated} = 1-\rho_{ae}/\rho_p$) of 0.85, 0.82 and 0.81 and an experimental superficial gas velocity (U) of 0.5, 0.21 and 0.39 m/s for TiO_2 (A), TiO_2 (R1) and TiO_2 (R2), respectively, the corresponding velocities (q) (Horio and Iwadate, 1996) are 0.24 m/s, 0.188 m/s, and 0.218 m/s, respectively.

A successive approximation method was applied to solve equation (19). Diameters of $d_a=310$ σm, $d_a=352$ σm and $d_a=298$ σm were found for the three different powders (TiO_2 (A), TiO_2 (R1) and TiO_2 (R2)), respectively. The numerical prediction of the agglomerate size (d_a) is a factor of 1520, 2213 and 1784 higher than the diameter of the primary particles (d_p) for the three powders TiO_2 (A), TiO_2 (R1) and TiO_2 (R2), respectively. These results are in accord with the agglomerates diameters (d_{pa}) estimated from equation (6), with a variation of 17 to 20%.

CONCLUSION

The disintegration of the cohesive structure in a fluidized bed was performed under a high gas velocity up to 4×10^6 times the velocity necessary for fluidizing the primary particles.

In the fluidized state, the experiments show that the exchange is carried out particularly between gas and the agglomerates formed from primary particles of different size and shape. There is a close correlation between the hydrodynamics and the local structure, controlled primarily by the van der Waals forces. The fluidized bed of agglomerates constitutes a new structure characterized by new physical properties of the agglomerates (ψ_a, ε, d_a). Indeed, this new hydrodynamic behavior can be classified in group B of Geldart's classification.

The integration of the flowability and the physical properties of the powders is an interesting way of describing the hydrodynamic behavior of these very cohesive powders.

This work constitutes a fundamental step in comprehending the behavior of cohesive powders in a fixed or fluidized bed. Indeed, these effects present a challenge due to the complexity of the microscopic processes such as the formation of agglomerates and the trajectory of gas within the solid structure.

The flow properties of the powders could not be predicted by only one indicator or inherent parameter describing the powders properties.

The connections of two or several flow tests are enough to predict the flow of powders: free flow, non-free flow or intermediate flow. However, in some categories of powders such as TiO_2 (nanometric powder) it is suitable to link all tests for different requests. Indeed, the cohesive character is established only under high external pressures. The distinction between the behavior of micronic and nanometric powders is an interesting area that needs to be further investigated.

NOMENCLATURE

A	Hamaker constant	J
C	Cohesion of powder	N/m^2
C_d	Drag coefficient	(-)
C_u	Index of uniformity	(-)
B	Boltzmann's constant	J/K
d_i	Average diameter in class i	m
d_p	Mean particule diameter	m
d_{pa}	Dynamic diameter of agglomerate (calculated by equation 6)	m
d_a	Calculated particle diameter of agglomerate (numerical approach)	m
E	Young's modulus	Pa
F	Force	N
F_c	Compressive resistance	N/m^2
F_{co}	Collision forces	N
FF_c	Parameter to characterize the flow properties	(-)
F_g	Gravitational force	N
F_{va}	Cohesive force	N
F_y	Drag force	N
g	Gravitational acceleration	$m.s^{-2}$
HR	Hausner's index	(-)
h	Planck's constant	J.s
K	Function of Poisson's ratio and Young's modulus	Pa^{-1}

M	Mass of the packed bed of particles	kg
m_i	Mass of agglomerate i (i = 1, 2)	kg
n	Function defined by equation 11	(-)
n_1	Function defined by equation 11a	(-)
Ni	Number of particles in class i	(-)
N_1	Index of refraction of particles	(-)
÷P	Total pressure drop in fluidized bed	Pa
q	Relative velocity of agglomerate	m/s
S	Cross-sectional area of the glass piston	m^2
S_s	Specific surface area	m^2/g
T	Temperature	K
U	Superficial gas velocity	m/s
U_{mfa}	Minimum apparent fluidization velocity	m/s
U_{mfc}	Minimum fluidization velocity calculated by equation (6)	m/s
V_t	Total volume of the packed bed of particles	m^3
z	Projected area of a sphere	m^2

Greek Letters

ζ	Angle of repose	(°)
ζ_d	Maximum compression displacement	m
η	Angle of slide	(°)
ι	Distance between agglomerates or particles	m
κ	Bed voidage	(-)
κ_1	Dielectric constant of particles	
$\kappa_{aerated}$	Aerated porosity of the bed of particles	(-)
$\mathring{U}_f$	Fluidized bed voidage	(-)
σ_g	Gas viscosity	$kg.m^{-1}.s^{-1}$
ψ_a	Agglomerate density	$kg.m^{-3}$
ψ_{ae}	Aerated powder bed density	$kg.m^{-3}$
ψ_g	Gas density	$kg.m^{-3}$
ψ_p	Particle density	$kg.m^{-3}$
ψ_t	Tapped density	$kg.m^{-3}$
$\mathring{u}$	Normal stress	Pa
$\mathring{u}_{sf}$	Normal stress (stationary flow)	Pa
$\mathring{u}_1$	Principal stress	Pa
ϑ	Shear stress	Pa
ϑ_{sf}	Shear stress (stationary flow)	Pa
τ_c	UV absorption frequency	s^{-1}
ε	Internal porosity	(-)
ϒ	Poisson's ratio	(-)

REFERENCES

Chirone, R., Massimilla, L. and S. Russo, Bubble-free fluidization of cohesive powder in an acoustic field, Chemical Engineering Science 48, p. 41-51 (1993).

Derjaguin, B., Untersuchungen über die Reibung und Adhäsion. Kolloid. Zeits., 69, p. 155 (1934).

Fatah, N. and Cavrois, V., Measurement of fluidization properties of fine particles and interaction with rheological parameters. Fluidisation IX, Engineering Foundation, Ed., Fan, L.S. and Knowlton, T., p. 277- 284, New York (1998).

Fatah, N., Pietrzyk, S. and Cavrois, V., Mesures de paramètres rhéologiques des poudres cohésives, 2ème Colloque Science et Technologie des Poudres, 3-5 mars Lyon, p. 283-290 (1998).

Fatah, N., Sanchez-Calvo, L., Effet de la pression acoustique sur la fluidisation des poudres cohèsives, 4ème colloque, Science et Technologie des Poudres, Récent progrès en Génie des Procédés 91 (2004).

Geldart, D., Types of gas fluidisation, Powder Technology 7, p. 285-292 (1973).

Horio, M. and Iwadate, Y., The prediction of sizes of agglomerates formed in Fluidized beds, Proc. of the 5th World Congress of Chem. Engineering, 2nd Intl. Particle Technology Forum V, p. 571 (1996).

Israelachvili, J. N., Intermolecular and Surface forces, Academic press, London (1985).

Jenike, A.W., Better design for bulk handling, Chem. Eng 175 (1954).

Khan, A. R. and Richardson, J. F., Pressure gradient and friction factor for sedimentation and fluidisation of uniform spheres in liquids, Chem. Eng. Sci. 45 (1), p. 255 (1990).

Krupp, H., Particle adhesion. Theory and experiment, Adv. Coll. Interf. Sci., 1, p. 111-239 (1967).

Leu, L. and Huang, C. T, Fluidization of cohesive powders in a sound waves vibrated fluidized bed, AIChE Sym. Ser. 90, p. 124-141 (1994).

Lifshitz, E. M., The theory of molecular attractive forces between solids, Soviet Phys. JETP (Engl. Transl.) 2, p. 73-83 (1956).

Nezzal, A., Etude de la fluidisation agitée des poudres fines, Thèse UTC (1996).

Pacek, W. and Nienow, A. W., Fluidization of fine and very dense hardmetal powders, Powder Technology 60, p. 145-158 (1990).

Perry, R. H. and Green, D., Perry's Chemical Engineers' Handbook 6th ed. McGraw Hill (1984).

Richardson, J. F. Incipient Fluidization and Particulate Systems. In: Davidson, J. F. and Harrison, D., Eds., Academic Press London (1971).

Russo, P., Chirone, R., Massimilla, L. and Russo, S., The influence of the frequency of acoustic waves on sound assisted fluidization of beds of fine particles, Powder Technology 82, p. 219-230 (1995).

Schlosser, F., Eléments de mécanique des sols, Presses de l'école National des Ponts et Chaussées 26 (1988).

Schulze, D., Appropriate devices for the measurement of flow properties for silo design and quality control, 3rd Euro. Symp. Storage and flow of particulate solids, PARTEC, Nuremberg/ Germany 21-23, p. 45-56 (1995).

Timoshenko, S. P. and Goodier, J. N., Theory of elasticity Mc Graw-Hill (1970).

Wen, C. Y. and Yu, Y. H., A generalized method for predicting the minimum fluidization velocity. A.I.Ch.E.Journal. 12, p. 610 (1966).

Wen, C. Y. and Yu, Y. H., Mechanics of fluidization., Chem. Prog. Symp. Ser. 62, p. 100-111 (1966).

Zhou, T. and Li, H., Estimation of agglomerate size for cohesive particles during fluidization, Powder Technology 101, p. 57-62 (1999).